Absolute Valued Message Passing-Based PAPR Reduction in OTFS under Fading Channel Conditions

Illuru Rajasekhar,
Department of Electronics and Communication Engineeing,
VELS University, Chennai, Tamil Nadu, India -600117.
gootyrajasekhar@gmail.com

M. Monisha,
Department of Electronics and Communication Engineeing,
VELS University, Chennai, Tamil Nadu, India -600117..
monisha.se@vistas.ac.in

2025 IEEE International Conference on Advanced Computing Technologies (ICACT) | 979-8-3315-9002-4/25/$31.00 ©2025 IEEE | DOI: 10.1109/ICACT67549.2025.11351506

***Abstract*— Orthogonal Time-Frequency Space (OTFS) modulation presents significant advantages over conventional modulations such as OFDM, particularly for high mobility communication environments, by functioning optimally within doubly dispersive channels. OTFS, however, carries an important drawback common to multicarrier modulations the high Peak-to-Average Power Ratio (PAPR) which contributes to diminished power amplifier efficiency and increased distortions caused by nonlinearity. This work proposes an Absolute Valued Message Passing (AVMP) detector, tailored for OTFS systems under fading channel environments. It is tested using Bit Error Rate (BER) and Complementary Cumulative Distribution Function (CCDF) of PAPR metrics through sophisticated MATLAB simulation under different Signal-to-Noise Ratios (SNR) and different orders of modulations (128-QAM, 256-QAM, 512-QAM). Results explicitly show that the AVMP detector consistently has better BER and significantly less PAPR than conventional techniques MP-OTFS, ZF-OTFS, conventional OTFS, and OFDM. These achievements confirm the competence of AVMP to upgrade OTFS modulation, significantly boosting communication reliability and efficiency for stochastic wireless environments.**

Keywords— OTFS, Absolute Valued Message Passing, PAPR, BER, CCDF, Fading Channels, QAM modulation

I. INTRODUCTION

Orthogonal Time-Frequency Space (OTFS) modulation is a strongly emerging method for next-generation wireless communication systems, especially for applications involving high mobility, e.g., vehicular communication, high-speed rail, and low-earth-orbit satellites. OTFS modulation naturally maps the information to the delay-Doppler domain, which offers better resilience against the negative effects of doubly dispersive channels exhibiting frequency and temporal selectivity [1], [2]. This resilience dramatically surpasses the conventional modulation schemes like Orthogonal Frequency Division Multiplexing (OFDM), which exhibit poor performance under high channel dynamics.

In spite of these benefits, OTFS modulation inherits one crucial drawback common to multicarrier modulation schemes the high Peak-to-Average Power Ratio (PAPR). PAPR is the proportion of the highest instantaneous signal power and average power, and an increased PAPR requires the power amplifier to operate under a significant input back-off (IBO), decreasing the overall power efficiency [3]. Additionally, high PAPR signals experience more non-linear distortion, thus causing regrowth in the spectra, an increased Bit Error Rate (BER), and a decreased overall system performance [4]. As a consequence, successfully countering the high PAPR has been necessary for realizing the full potential of OTFS modulation.

The conventional methods employed for PAPR minimization in OFDM systems under fading channel, i.e., clipping and filtering, SLM, and PTS, have been explored for OTFS modulations to different extents of success. Though clipping and filtering are easy to implement, they introduce distortion and make it inefficient for practical implementation at high-performance applications [5]. Methods like SLM and PTS are efficient PAPR suppressors when they adaptively adjust the phases of the signal being transmitted, but they add high complexity through numerous reverse transforms and searches for selecting the best signal [6] [7].

Recent studies have branched out beyond traditional techniques, investigating sophisticated optimization and machine learning methods for effectively decreasing PAPR for OTFS systems over the fading channel. Some hybrid techniques combining traditional methods and optimization and learning techniques like Genetic Algorithms (GA), Particle Swarm Optimization (PSO), and Grey Wolf Optimization (GWO) have opened significant doors to balancing between system performance and computational complexity [8]. Moreover, machine learning-based techniques, specifically based on neural network-based solutions, have drawn significant interest due to their ability to learn adaptively optimal signal transforms achieving minimum PAPR using much less complexity [9] [10].

A key concern when analyzing PAPR reduction methods for OTFS modulation is the trade-off among PAPR reduction for fading channel, degradation of the signal quality, and computational complexity. Some techniques that provide excellent PAPR reduction may impose increased computational complexity or affect other fundamental metrics for communication like BER and spectral efficiency. Hence, modern literature focuses on hybrid techniques, combining traditional and contemporary computational techniques for maintaining an effective balance between the trade-offs mentioned above [11].

Besides, the performance comparison of PAPR reduction methods under fading channel is greatly dependent on common measures involving the Complementary Cumulative Distribution Function (CCDF) of PAPR, BER analysis, and the rate of spectral efficiency. Comparisons would be carried out under standard channel models, e.g., the 3GPP-specified

wideband fading channel, synthetic multipath fading channels, and real-world vehicular and satellite communication environments, so that there is practical validity and relevance to the methods under investigation [12].

In addition, the design and implementation of real-time implementable PAPR reduction schemes under fading channel has been gaining prominence because of changing communication standards and deployment situations that require high data rate and reliability. Real-time implementable schemes require not only significant PAPR reduction but also computational simplicity and low latency. Hence, research currently also aims at hardware-friendly implementation and optimization for embedding within conventional system hardware [13].

While considerable progress has been made in developing efficient PAPR reduction techniques for OTFS modulation, gaps remain. Most notably, a comprehensive comparative analysis incorporating recent advancements, particularly in the context of computational complexity and adaptability under varying communication environments, is still necessary. Moreover, exploring novel hybrid frameworks integrating classical, optimization-based, and machine-learning-driven approaches could pave the way toward universally robust and practically implementable solutions [14].

II. System's Overview

The fundamental concepts in OTFS system and input-output relations in delay-doppler domain are discussed in this section. OTFS modulation corresponding to the proposed multiple carrier time-frequency (TF) modulation is shown in Fig. 1. While describing this OTFS model the notation of [15] [16] and [1] was used.

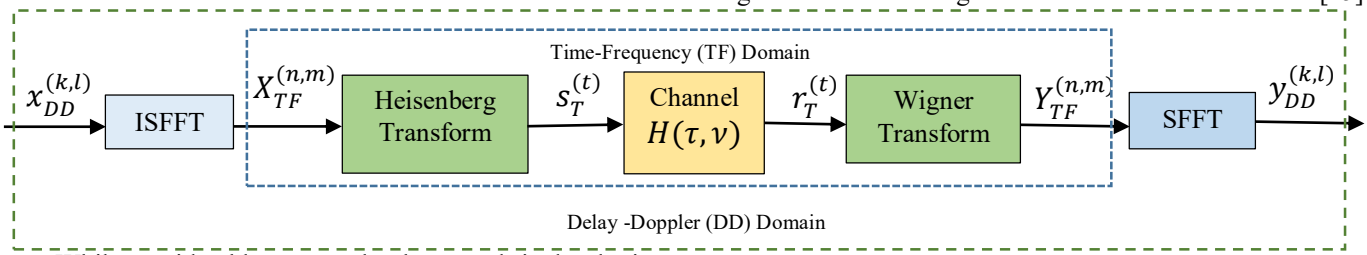

Fig. 1 Block diagram of modulation scheme in OTFS system

At both the transmitter and receiver, a sequence of two-dimensional transformations is performed to produce OTFS modulation. The modulator first converts the information symbols $x_{DD}^{(k,l)}$ from the DD domain to samples $X_{TF}^{(n,m)}$ in the TF domain with Inverse Symplectic Finite Fourier Transform (ISFFT). Then, the time domain signal $s_T^{(t)}$ transmitted via the wireless channel is obtained by taking the Heisenberg Transform (HT) on $X_{TF}^{(n,m)}$.

A. Genaral OTFS Scheme

Let us assume a information packets of NXM taken from a modulation alphabet that is made up of QAM symbols of size Q_A. It is possible to organize these QAM symbols on 'ψ', the DD grid as $x_{DD}^{(k,l)}$. The OTFS transmitter uses the ISFFT for conversion of symbols $x_{DD}^{(k,l)}$ into NXM time-frequency grid 'Γ' samples $X_{TF}^{(n,m)}$, according to equation (1).

$$X_{TF}^{(n,m)} = \frac{1}{\sqrt{NM}} \sum_{k=0}^{N-1} \sum_{l=0}^{M-1} x_{DD}^{(k,l)} W_N^{-kn} W_M^{ml} \tag{1}$$

where, $m = 0,1,\ldots..M-1$, $n = 0,1,\ldots.N-1$, $W_N^{-kn} = e^{j2\pi\left(\frac{nk}{N}\right)}$ and $W_M^{ml} = e^{j2\pi\left(\frac{-ml}{M}\right)}$.

A transmitting waveform $g_{(t)}^T$ in a TF modulator uses samples of the transform $X_{TF}^{(n,m)}$ with in a $s_T^{(t)}$ which is a waveform in continuous domine with respect to equation (2).

$$s_T^{(t)} = \sum_{n=0}^{N-1} \sum_{m=0}^{M-1} X_{TF}^{(n,m)} g_{(t)}^T (t-nT) e^{j2\pi m\Delta f(t-nT)} \tag{2}$$

With respect to the above reference, equation (2) is widely used as well-known Heisenberg transform [17], in this article mentioned as $g_{(t)}^T$

B. Wireless transmission and reception

Consider 'τ' as a delay and 'ν' as doppler with the response in discrete domine developed as baseband channel $H(\tau,\nu)$, which sending the continuous signal $s_T^{(t)}$ as an dependent time channel. $r_T^{(t)}$, from equation (3) has to represent in the TF domain.

$$r_T^{(t)} = \iint H(\tau,\nu)\, s_T^{(t)}(t-\tau) e^{j2\pi\nu(t-\tau)} d\tau d\nu \tag{3}$$

From the shown above equation (3), $S^{(t)}$ is used to indicate a Heisenberg transform. The DD domain channels are modelled with required parameters for the measure of reflections in channel and associated delay dopplers should get minimized. The sparsely domain presentation represented in equation (4) for the give channel.

$$H(\tau,\nu) = \sum_{i=1}^{PP} H_i \delta(\tau-\tau_i)\delta(\nu-\nu_i) \tag{4}$$

where, PP indicated the paths of propagation counts, generally mentioned from the Heisenberg transform in the DD domain as reflected by the delta $\delta(\cdot)$ function in discrete domain with i^{th} direction.

For i^{th} path, the delay and continues taps are indicated in DD domain and given in equation (5).

$$\tau_i = \frac{l_{\tau_i}}{M\Delta f}, \qquad \nu_i = \frac{K_{\nu_i} + \Delta k_{\nu_i}}{NT} \tag{5}$$

where, l_{τ_i}, K_{ν_i} are integers and $-\frac{1}{2} < k_{\nu_i} < \frac{1}{2}$.

The delay tap index l_{τ_i} and Doppler tap index K_{ν_i} are associated with (discrete delay) τ_i and Doppler effected ν_i.

Δk_{v_i} shall hereafter be named as slight Doppler and K_{v_i} as the nearest Doppler tap [18]

III. Proposed PAPR Reduction Technique using Absolute Valued Message Passing Detector

To address the limitations of high PAPR in OTFS systems, particularly under fading channels, we introduce the Absolute Valued Message Passing (AVMP) detector. This technique combines the denoising strength of message passing with a nonlinear transformation leveraging absolute values, thereby offering a robust and low-complexity approach to mitigate peak power issues without compromising symbol recovery or increasing BER [19]. The approach is inspired by iterative belief propagation but integrates a non-saturating rectifier that maintains signal sparsity and enhances convergence stability under channel impairments. In the study of a more generalized LTV channel, we find that the propagated signal undergoes fast fading $\gamma^i(t)$ along every path of propagation, and that the amplitude and phase of this fading are factors of time. Assuming no loss of generality, the following equation mathematically represents the received signal, designated as $c(t)$ given in equation (6)

$$c(t) = \sum_{i=1}^{z} \gamma^i(t) r(t - \tau_i) e^{j2\pi v_i (t-\tau_i)} + p(t) \qquad (6)$$

The $\gamma^i(t)$ function will inevitably disrupt the WH basis's orthogonality and have a significant effect on the IO relationship in the DD space.

The Input Output (IO) relation might have multiple representations, which are defined through propagation of electromagnetic waves in different contexts. If every path possesses unique characteristics of propagation.

Furthermore situation, if the environment surrounding the antenna changes over time, the signal that bounces off multiple surfaces is assumed to experience the same dispersion, making it difficult to differentiate $\gamma(t)$. Illustrations can be located within the domain of reentry communication. In addition, the system's response for a single pulse during time (t) or (t-τ) discovers if anything has changed in $\gamma(t)$. When the signal encounters $\gamma(t)$ and thereafter travels through multiple paths, it is important to take into account the translation, or the reverse scenario. The end outcomes in many scenarios can be deduced using a comparable approach, relying on the necessary definition..

$$C_{pq,p'q'} = \sum_{i=1}^{Z} \int_t \gamma^i(t) g_{p'q'}(t - \tau_i) e^{j2\pi v_i (t-\tau_i)} g^*_{pq}(t) dt \qquad (7)$$

Deriving $C_{pq,p'q'}$ directly can be troublesome due to the presence regarding the integrated operator, even in cases when explicit features of $g(t)$ and $\gamma(t)$ are provided. In order to address the above issue, we employ a discretization technique that relies on the characteristics of the Weyl-Heisenberg Basis foundation.

Using the comprehensive WH basis, it is possible to reconstruct the signal.

$$f(t) = \sum_{p,q} \langle f(t), g_{pq}(t) \rangle g_{pq}(t) \qquad (8)$$

The expression for $g_{pq}(t)$ as given in equation (8) with the inclusion of delay and Doppler τ_i and v_i respectively, can be reformulated as follows:

$$g_{pq}(t - \tau) e^{j2\pi v (t-\tau)} = \sum_{p',q'} H^i_{pq,p'q'} g_{p'q'}(t) \qquad (9)$$

where,

$$H^i_{pq,p'q'} = A_g\big((p-p')T - \tau_i, (q-q')\Delta f - v_i\big). e^{j2\pi(q'\Delta f + v_i)((p-p')T - \tau_i)} e^{j2\pi v p' T} \qquad (10)$$

By replacing the reconstructed value in equation (10), the value of $C_{pq,p'q'}$ can be computed as equation

$$\begin{aligned} C_{pq,p'q'} &= \langle \sum_{i=1}^{z} \gamma^i(t) \sum_{p'',q''} H^i_{p'q',p''q''} g_{p''q''}(t), g_{pq}(t) \rangle \\ &= \sum_{i=1}^{z} \sum_{p'',q''} H^i_{p'q',p''q''} \langle \gamma^i(t) g_{p''q''}(t), g_{pq}(t) \rangle \end{aligned} \qquad (11)$$

Equation (11) specifies that the $C_{pq,p'q'}$ can be expressed as the sum of inner products and their corresponding $H^i{}_{pq,p'q'}$. Thus, the integral is simplified by removing the consequences of doppler and delay, resulting in an understated name for the inner product. The dispersion at every point of the TF lattice is described by the Channel Impulse Response (CIR) of $\gamma^i(t)$, which is represented by the inner products. The CIR of time-variant fading γ(t) among the time-frequency lattice can be characterized as in equation

$$\langle \gamma(t) g_{p'q'}(t), g_{pq}(t) \rangle = \begin{cases} \frac{1}{Q} \sum_{u=0}^{Q-1} \bar{\gamma}_p(u) e^{-j2\pi \frac{u}{Q}(q-q')} & p = p' \\ 0 & otherwise \end{cases} \qquad (12)$$

where, the $\bar{\gamma}_p(u)$ represents the initial samples of $\gamma(t)$ using a sampling rates of $1/Q\Delta f$ during the period of p^{th} symbol.

Equation (12) gives a clear elucidation of the connection between the WH basis. When q=q', the CIR represents the component at the point of zero frequency. Additionally, when the q' signal changes, the CIR will also shift in a circular manner along the frequency axis. For a given constant value of p and q, the frequency response is obtained by performing a circular convolution.

From equation (11), PAPR mathematically represented as equation (13).

$$PAPR = \frac{max_{0 \le n < N} |C_{pq,p'q'}|^2}{\mathbb{E}\left[|C_{pq,p'q'}|^2\right]} \qquad (13)$$

The Complementary Cumulative Distribution Function (CCDF) of PAPR is the probability that PAPR exceeds a given threshold *'γ(t)'* as given in equation (14)

$$CCDF(\gamma) = \Pr(PAPR > \gamma)$$

$$CCDF_G^{\gamma} = 1 - (1 - e^{-\gamma})^N \quad (14)$$

where, $CCDF_G^{\gamma}$ represents complex Gaussian symbols with high oversampling, the theoretical CCDF. The AVMP suppresses outlier peaks, effectively minimizing high PAPR instances and given in equation (15)

$$PAPR_{AVMP} = \frac{max\left|C_{pq,p'q'_{AVMP}}\right|^2}{\mathbb{E}\left[\left|C_{pq,p'q'_{AVMP}}\right|\right]^2} \quad (15)$$

IV. Results and Discussions

In this section validate the effectiveness of suggested AVMP OTFS detector for rapid fading channels under the aspect of PAPR and BER. Simulation setup used for the analysis of this research article used MATLAB R2024a to study the performance of AVMP detector, i.e., BER and Peak-to-Average Power Ratio (PAPR). Simulation parameters were judiciously selected to ensure comprehensive study under real-world conditions. To compare BER, the simulation took into account 256 number of subcarriers(NoS) for 10000 symbols and used 128, 256 and 512-QAM order (QAMORD). The Signal-to-Noise Ratio (SNR) was varied between 2 dB and 14 dB at an increment of 2 dB. Simulation was done by adding additive white Gaussian noise (AWGN) to the transmitted signals and calculated resultant BER for every SNR. For the comparison of PAPR reduction, 256 subcarriers and 20,000 symbols and 128, 256 and 512-QAM modulation was used. An oversampling factor of 4 was utilized for obtaining the correct values for PAPR under fading. The CCDF of PAPR was calculated for analyzing the PAPR exceedance probability for different PAPR values, which gave clear comparative insights for assessing each method's merits and demerits. The efficiency of the suggested technique was compared to existing methods, Zero Forcing (ZF) [20], Message passing detector [21], general OTFS [22] and OFDM [23] are employed.

The Fig. 2 plots the Bit Error Rate (BER) against the Signal-to-Noise Ratio (SNR) for comparison between the suggested AVMP detector and traditional methods like MP-OTFS, ZF-OTFS, standard OTFS, and OFDM. It can be seen that there exists a clear trend through which the BER steadily reduces as the SNR increases for all the methods that have been tested, meaning better transmission reliability and increased data purity for stronger signals against noise.

Out of the compared methods, the suggested AVMP detector has the minimum BER for the entire set of SNR values under consideration. This better performance underscores the capability of the AVMP detector to successfully tackle fading channel conditions. Indeed, MP-OTFS closely tracks the performance of the AVMP detector but has an ever so slightly higher rate of errors, stressing the fact that there is a real advantage offered by the use of AVMP.

The ZF-OTFS, conventional OTFS, and OFDM schemes always exhibit higher BER, particularly at lower values of SNR. This reflects their comparative shortcomings under difficult fading situations, and hence are less desirable for situations where stringent control over low-error rates is necessary. While the BER plots converge under higher SNR values (for example, 12–14 dB), the advantage of the AVMP detector persists through its ability to obtain consistently better error rates.

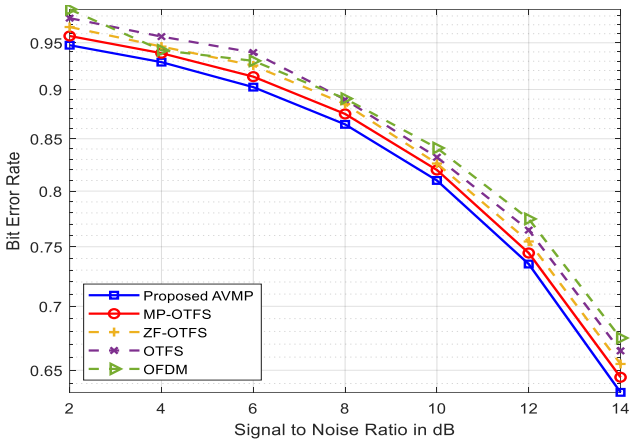

Fig. 2: BER Vs SNR (NoS-256 QAMORD-128)

In Fig. 3, for 256 subcarriers and 256-QAM, the suggested Absolute Valued Message Passing (AVMP) detector reliably achieves the lowest BER over the overall SNR range, which is 2–14 dB. This performance greatly exceeds other techniques under comparison, i.e., Message Passing OTFS (MP-OTFS), Zero Forcing OTFS (ZF-OTFS), conventional OTFS, and OFDM. As SNR increases, BER for all techniques decreases, but the AVMP approach has a significant advantage, and, especially between 10–14 dB, the difference between BER performance and other techniques becomes significant. This proves that AVMP is greatly effective for preserving signal quality and decreasing the rate of errors under fading channel and higher-order modulation.

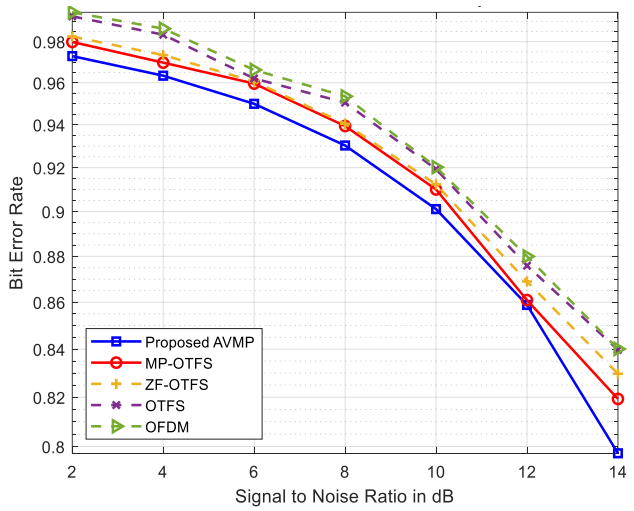

Fig. 3: BER Vs SNR (NoS-256 QAMORD-256)

In the Fig. 4, the modulation order is increased to 512-QAM, maintaining the number of subcarriers at 256. Due to the higher modulation order, the overall BER values are higher compared to the 256-QAM scenario, reflecting increased susceptibility to noise and channel impairments. However, the proposed AVMP detector continues to significantly outperform other detection methods. Notably, while all methods show a decreasing trend in BER with

increasing SNR, the AVMP consistently demonstrates the lowest BER, especially evident at higher SNR levels. This clearly emphasizes the robustness and effectiveness of the AVMP detector, even in conditions involving higher-order modulations that inherently present more challenges in terms of error rates.

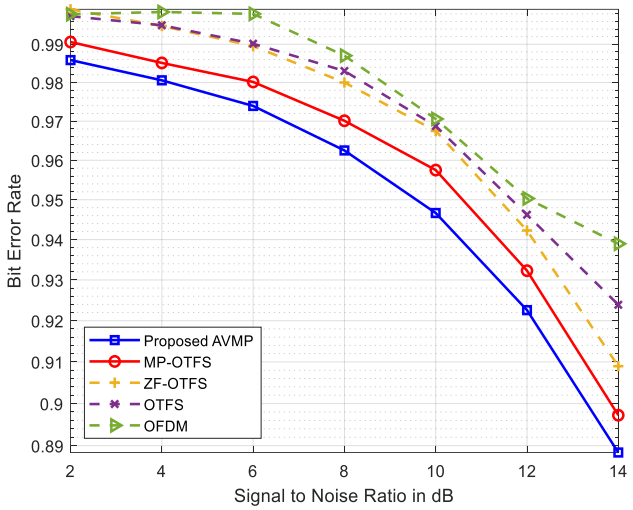

Fig. 4: BER Vs SNR (NoS-256 QAMORD-512)

All the figures underline the effectiveness of the proposed AVMP detector. While higher-order modulation generally elevates the BER, the AVMP approach successfully maintains the best performance, demonstrating robustness and improved reliability in communication over fading channels irrespective of the modulation complexity.

Further, Peak-to-Average Power Ratio (PAPR) analysis using the Complementary Cumulative Distribution Function (CCDF) for the proposed Absolute Valued Message Passing (AVMP) detector compared against conventional techniques: OTFS, MP-OTFS, ZF-OTFS, and OFDM, under varying QAM modulation orders (128,256,512) while maintaining 256 subcarriers.

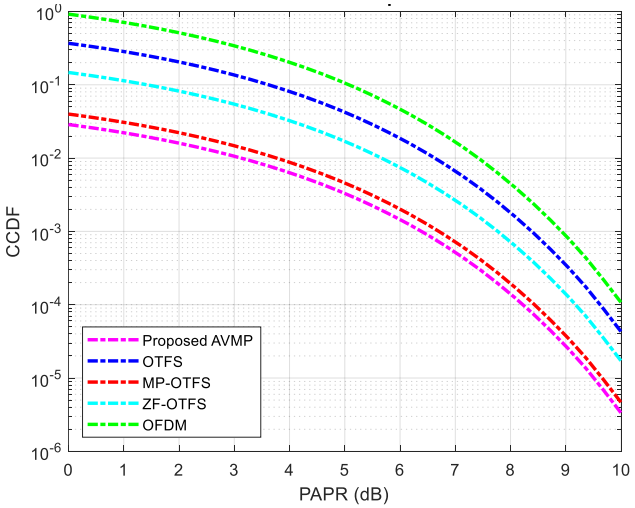

Fig. 5: PAPR comparison with CCDF (NoS-256 QAMORD-128)

In Fig. 5, with a lower modulation order (128-QAM), the proposed AVMP demonstrates the lowest CCDF values across the entire PAPR range (0–10 dB). This indicates that the AVMP method has significantly reduced the probability of signals exceeding high PAPR thresholds compared to other approaches. OFDM exhibits the highest CCDF values, implying the poorest performance in PAPR reduction. OTFS, MP-OTFS, and ZF-OTFS perform better than OFDM but are consistently outperformed by AVMP, clearly showing AVMP's effectiveness in minimizing high power peaks.

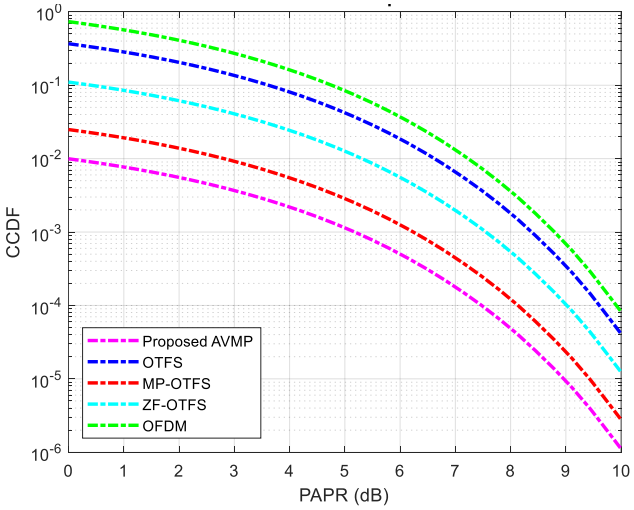

Fig. 6: PAPR comparison with CCDF (NoS-256 QAMORD-256)

In Fig. 6, As the modulation order increases to 256-QAM, the general trend remains consistent with the previous observation: the AVMP method continues to provide the best PAPR performance. Compared to other methods, the AVMP still exhibits the lowest CCDF values across all tested PAPR thresholds, reinforcing its efficiency. Although all methods experience relatively higher CCDF values due to increased modulation complexity, the AVMP approach still significantly mitigates this increase, maintaining superior performance over OTFS variants and OFDM.

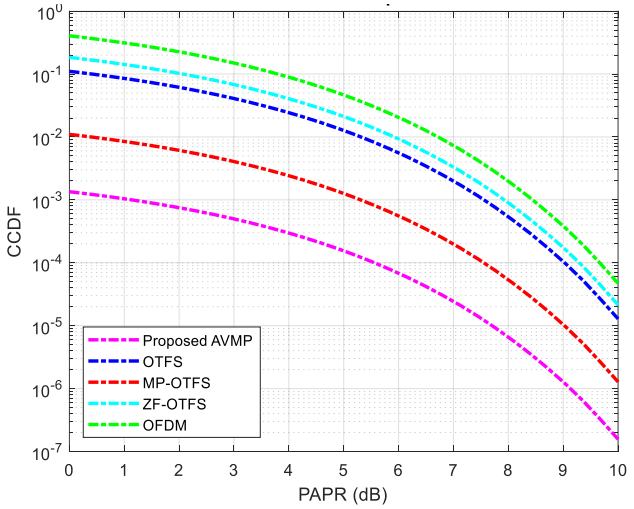

Fig. 7: PAPR comparison with CCDF (NoS-256 QAMORD-512)

In Fig. 7, the final scenario using a higher modulation order of 512-QAM, the CCDF values slightly increase for all compared techniques, reflecting higher susceptibility to peaks due to increased complexity. However, AVMP still clearly demonstrates the lowest CCDF values, underscoring its continued effectiveness in managing and significantly reducing PAPR even under challenging modulation

conditions. OFDM consistently presents the highest CCDF, highlighting its inherent limitations in high-order modulation scenarios. OTFS-based variants perform better than OFDM but are clearly less efficient compared to the AVMP method.

Across all examined modulation complexities, the proposed AVMP consistently demonstrates the best PAPR reduction performance. It robustly manages peak power issues and significantly reduces the probability of exceeding high PAPR thresholds, thereby providing substantial benefits for practical applications where amplifier efficiency and nonlinear distortion minimization are critical considerations.

V. Conclusion and Future Scope

With efficient reduction of Bit Error Rate (BER) and Peak-to-Average Power Ratio (PAPR) for varied fading channel conditions and complexity modulations, this work established that the proposed Absolute Valued Message Passing (AVMP) detector significantly improves the performance of OTFS modulation. The AVMP was frequently seen performing more effectively than conventional detection methods, thus emphasizing its robustness and practical use within existing communication systems requiring high reliance and effectiveness..

Future work can pursue the integration of the AVMP detector using machine-learning-based adaptive techniques, continuing to fine-tune the behavior for different operational environments. Real-time implementation and large-scale field work under realistic high-mobility environments like vehicular and satellite communications could confirm and further advance the practical viability of the new method. Exploration of hybrid frameworks blending the use of AVMP and other types of optimization techniques, and detailed comparative studies taking complexity factors into account, are likely ways for realizing universally reliable and implementable OTFS solutions.

VI. References

[1] R. Hadani, S. Rakib, M. Tsatsanis, A. Monk, A. Goldsmith, F. M. A and R. Calderbank, "Orthogonal Time Frequency Space Modulation," in *2017 IEEE Wireless Communications and Networking Conference (WCNC)*, San Francisco, CA, USA, 2017.

[2] Z. Wei, W. Yuan, S. Li, J. Yuan, G. Bharatula and R. Hadani, "Orthogonal Time-Frequency Space Modulation: A Promising Next-Generation Waveform," *IEEE Wireless Communications,* vol. 28, no. 4, pp. 136-144, 2021.

[3] Y. Rahmatallah and S. Mohan, "Peak-To-Average Power Ratio Reduction in OFDM Systems: A Survey And Taxonomy," *IEEE Communications Surveys & Tutorials,* vol. 15, no. 4, pp. 1567-1592, 2013.

[4] A. Kumar, N. Gaur, S. Chakravarty and A. Nanthaamornphong, "Reducing the PAPR of OTFS Modulation Using Hybrid PAPR Algorithms," *Wireless Personal Communications,* vol. 133, p. 2503–2523, 2023.

[5] S. H. Han and J. H. Lee, "An overview of peak-to-average power ratio reduction techniques for multicarrier transmission," *IEEE Wireless Communications,* vol. 12, no. 2, pp. 56-65, 2005.

[6] J. Armstrong, "Peak-to-average power reduction for OFDM by repeated clipping and frequency domain filtering," *Electronics Letters,* vol. 38, no. 5, 2002.

[7] J.-C. Chen, "Partial Transmit Sequences for Peak-to-Average Power Ratio Reduction of OFDM Signals With the Cross-Entropy Method," *IEEE Signal Processing Letters,* vol. 16, no. 6, pp. 545 - 548, 2009.

[8] M. H. Aghdam and A. A. Sharifi, "A novel ant colony optimization algorithm for PAPR reduction of OFDM signals," *International Journal of Communication Systems,* vol. 34, no. 1, 2021.

[9] E. Abdullah, K. Dimyati, W. N. W. Muhamad, N. I. Shuhaim, R. Mohamad and N. M. Hidayat, "Deep learning based asymmetrical autoencoder for PAPR reduction of CP-OFDM systems," *Engineering Science and Technology, an International Journal,* vol. 50, p. 101608, 2024.

[10] B. S. d. C. d. Silva, V. D. P. Souto, R. D. Souza and L. L. Mendes, "A Survey of PAPR Techniques Based on Machine Learning," *Sensors,* vol. 24, no. 6, p. 1918, 2024.

[11] S. R. Kondamuri and A. Sundru, "Performance analysis of hybrid PAPR reduction technique for LTE uplink communications," *Physical Communication,* vol. 29, pp. 103-111, 2018.

[12] J. Wang, C. Yang, Z. Pan and S. Shimamoto, "Optimization on OTFS Modulation Channel Estimation Path Employing CNN-based Self-Adjustment Model," in *2022 IEEE International Conference on Communications Workshops (ICC Workshops)*, Seoul, Korea, 2022.

[13] M. Isik, M. Nkomo, A. Das and K. R. Dandekar, "FPGA Implementation of OTFS Modulation for 6G Communication Systems," in *2023 IEEE Future Networks World Forum (FNWF)*, Baltimore, MD, USA, 2023.

[14] "PAPR analysis in OTFS using the centre phase sequence matrix based PTS method," *Results in Optics,* vol. 15, p. 100664, 2024.

[15] P. Raviteja, K. T. Phan, Y. Hong and E. Viterbo, "Interference Cancellation and Iterative Detection for Orthogonal Time Frequency Space Modulation," *IEEE Transactions on Wireless Communications,* vol. 17, no. 10, pp. 6501-6515, 2018.

[16] P. Raviteja, K. T. Phan, Q. Jin, Y. Hong and E. Viterbo, "Low-Complexity Iterative Detection for Orthogonal Time Frequency Space Modulation," in *2018 IEEE Wireless Communications and Networking Conference (WCNC)*, Barcelona, Spain, 2018.

[17] V. Labunets, E. Rundblad-Labunets, J. Astola and K. Egiazarian, "Fast n-D Fourier-Heisenberg-Weyl transforms," in *2000 IEEE International Conference on Acoustics, Speech, and Signal Processing*, Istanbul, Turkey, 2000.

[18] D. Tse and P. Viswanath, Fundamentals of Wireless Communication, U.K., Cambridge: Cambridge Univ. Press, 2005.

[19] G. T. Vasu, S. Fiza, C. Suheil, S. I. N and P. V. V. Reddy, "OTFS Modulation Characterizations Over Rapid Fading Channel," in *2024 International Conference on Recent Innovation in Smart and Sustainable Technology (ICRISST)*, Bengaluru, India, 2024.

[20] Y. Liu, "A Massive MIMO Signal Detection Method Based on ZF Method," in *2021 5th International Conference on Imaging, Signal Processing and Communications (ICISPC)*, Kumamoto, Japan, 2021.

[21] X. Li, W. Yuan and Z. Li, "Hybrid Message Passing Detection for OTFS Modulation," in *2023 IEEE Wireless Communications and Networking Conference (WCNC)*, Glasgow, United Kingdom, 2023.

[22] Y. Wang, S. Han, B. Abderrahim, C. Li and W. Meng, "An Improved OTFS Transmission Frame Structure Design for PAPR Reduction," in *2024 20th International Conference on Wireless and Mobile Computing, Networking and Communications (WiMob)*, Paris, France, 2024.

[23] Vincent and A. Suhartomo, "Evaluation of BER Performance for M-Ary QAM OFDM Through Wireless Channel by Controlling PAPR at the Transmitter," in *2020 12th International Conference on Information Technology and Electrical Engineering (ICITEE)*, Yogyakarta, Indonesia, 2020.